INTERNATIONAL JOURNAL FOR NUMERICAL METHODS IN ENGINEERING
Int. J. Numer. Meth. Engng (2008)
Published online in Wiley InterScience (www.interscience.wiley.com). DOI: 10.1002/nme.2404

The method of fundamental solutions applied to the calculation of eigensolutions for 2D plates

Carlos J. S. Alves and Pedro R. S. Antunes*, †

CEMAT, Department of Mathematics, Instituto Superior Técnico, Av. Rovisco Pais 1, 1049-001 Lisboa, Portugal

SUMMARY

In this paper we study the application of the method of fundamental solutions (MFS) to the numerical calculation of the eigenvalues and eigenfunctions for the 2D bilaplacian in simply connected plates. This problem was considered in Kang and Lee (*J. Sound Vib.* 2001; **242**(1):9–16) using wave-type functions and in Chen *et al.* (*Eng. Anal. Boundary Elem.* 2004; **28**:535–545) using radial basis functions for circular and rectangular domains. The MFS is a mesh-free method that was already applied to the calculation of the eigenvalues and eigenfunctions associated with the Laplace operator (cf. *Appl. Math. Lett.* 2001; **14**(7):837–842; *Eng. Anal. Boundary Elem.* 2005; **29**(2):166–174; *Comput. Mater. Continua* 2005; **2**(4):251–266). The application of this method to the bilaplace operator was already considered in Chen and Lee (*ECCOMAS Thematic Conference on Meshless Methods*, Lisbon, 2005) for multiply connected domains, but only for simple shapes. Here we apply an algorithm for the choice of point-sources, as in Alves and Antunes (*Comput. Mater. Continua* 2005; **2**(4):251–266), which leads to very good numerical results for simply connected domains. A main part of this paper is devoted to the numerical analysis of the method, presenting a density result that justifies the application of the MFS to the eigenvalue biharmonic equation for clamped plate problems. We also present a bound for the eigenvalues approximation error, which leads to an *a posteriori* convergence estimate. Copyright © 2008 John Wiley & Sons, Ltd.

Received 8 May 2007; Revised 16 March 2008; Accepted 16 May 2008

KEY WORDS: eigensolutions; plate problem; method of fundamental solutions

*Correspondence to: Pedro R. S. Antunes, CEMAT, Department of Mathematics, Instituto Superior Técnico, Av. Rovisco Pais 1, 1049-001 Lisboa, Portugal.
†E-mail: pant@math.ist.utl.pt

Contract/grant sponsor: FCT-POCTI/FEDER; contract/grant numbers: POCTI-MAT/34735/00, POCTI-MAT/60863/2004, POCTI-ECM/58940/2004, NATO-PST.CLG.980398
Contract/grant sponsor: Fundação para a Ciência e Tecnologia; contract/grant number: SFRH/BD/19879/2004

1. INTRODUCTION

The determination of the eigenvalues and eigenfunctions associated with elliptic operators in a bounded domain Ω is a well-known problem with applications in engineering, for instance, in acoustics. In some simple situations explicit formulae for eigenvalues and eigenfunctions are available; however, when the shape is non-trivial the use of a numerical method for partial differential equations (PDEs) is required. Standard finite difference method (FDM), finite element method (FEM) or boundary element method (BEM) can produce fairly good results when dealing with rather general shapes. These classical methods require significant computational efforts: in the construction of the mesh and the associated rigid matrix, in the case of FDM/FEM, and in the integration of weakly singular kernels in the case of BEM (e.g. [1]). These mesh/integration efforts try to avoid ill-conditioned matrices that arise in global approximation methods, such as the methods of particular solutions (cf. [2]). On the other hand, the methods using particular solutions present excellent results with small ill-conditioned matrices, which could only be achieved in classical methods by using large matrices (especially for higher eigenvalues, since the mesh should follow the higher oscillations).

In this paper, we study the application of a method of particular solutions, which is usually known as the method of fundamental solutions (MFS), to solve the eigenvalue problem for the biharmonic operator, in the case of a simply connected clamped plate. The MFS has been mainly applied to boundary problems in PDEs, starting in the 1960s (e.g. [3]). This method has been applied to solve boundary problems in several linear PDEs, where the fundamental solution (e.g. Poisson or Helmholtz equations) or fundamental tensor (e.g. Navier or Stokes systems) is known (e.g. [3–6]). The application of the MFS to the calculation of the eigenfrequencies (a membrane problem—Laplace eigenvalues) was introduced by Karageorghis [4] and applied only for very simple shapes. It was shown that the MFS performance was better than the BEM used by De Mey [1]. In a previous paper [7] we have shown that the MFS is also a reliable method, using a particular choice of point-sources, for a general class of simply connected bounded domains. The MFS presented very good results in the calculation of eigenfrequencies and eigenmodes. The application of the MFS for the eigencalculation with multiply connected domains and simple geometries was also considered in [8]. In this case, spurious solutions also appear and to filter them out they applied the singular value decomposition and the Burton and Miller method. For the treatment of the spurious eigenvalue problems, see also [9]. The application of other meshless methods to the determination of eigenfunctions and eigenmodes has also been subject to recent research, mainly using radial basis functions (e.g. [10]). A similar type of meshless method, a Trefftz-type method, such as the method of particular solutions that dates back to the 1960s (cf. [11]) was recently recovered by Betcke and Trefethen (cf. [2]) to calculate eigenvalues of the Laplace operator. In this method, the particular solutions are specially adapted to polygonal shapes. The plate problem was already considered using mesh-free methods, for instance, Kang and Lee proposed a method based on non-dimensional influence functions (cf. [12]). That method results in spurious solutions that need a special treatment. Later, Chen *et al.* proposed a method based on radial basis functions and made an analytical study for the circular clamped plate (cf. [13]), and recently in [14] a regularized meshless method, similar to the MFS, was considered for the Helmholtz equation. The plate problem with different types of boundary conditions was studied in [15], where circular domains were considered.

In this paper, we consider the application of the MFS to simply connected clamped plate shapes (for the multiple connected case, see, e.g. [16, 17]). The first part of this paper consists in

DOI: 10.1002/nme

presenting theoretical justification for the application of the MFS, by first proving a density result in Section 2 using a sum of single- and double-layer potentials. In Section 3 we consider the implementation of an algorithm based on MFS (following [7]) that applies for general plates, since for non-trivial shapes the choice of the source-points is important to ensure stable and accurate approximations of the eigenvalues. On the basis of the approximations of the eigenvalues, we apply an MFS algorithm to obtain the associated eigenmodes. In Section 3 we also present an *a posteriori* error bound for the eigenvalues, which allows one to control the accuracy of the MFS approximations. Finally, in Section 4 we present some numerical results to illustrate the performance of the proposed method.

2. THE PLATE EIGENVALUE PROBLEM

Let $\Omega \subset \mathbb{R}^2$ be a bounded simply connected domain with regular boundary $\partial\Omega$. We will consider the 2D eigenvalue problem for the bilaplacian operator Δ^2 with Dirichlet boundary conditions, corresponding to a clamped plate, for simplicity (with appropriate changes other boundary conditions could be considered).

It is clear that the eigenvalue problem is equivalent to finding the frequencies λ that satisfy the biharmonic eigenvalue problem, i.e. there exists $u \not\equiv 0$ such that

$$\begin{cases} \Delta^2 u - \lambda^4 u = 0 & \text{in } \Omega \\ u = 0 & \text{on } \partial\Omega \\ \partial_n u = 0 & \text{on } \partial\Omega \end{cases} \tag{1}$$

where ∂_n stands for the normal derivative (the normal vector n points outside the domain Ω). If a pair (λ, u) satisfies problem (1), then we say that λ is an eigenfrequency and the non-null u is an eigenmode—this corresponds to recover the resonance frequencies $\lambda > 0$ associated with a particular shape of a plate Ω.

A fundamental solution Φ_ω of the biharmonic eigenvalue operator verifies $-(\Delta^2 - \omega^4)\Phi_\omega = \delta$ (where δ stands for the Dirac delta distribution). In the 2D case, we consider

$$\Phi_\omega(x) = \frac{\mathrm{i}}{8\omega^2}(H_0^{(1)}(\mathrm{i}\omega|x|) + H_0^{(2)}(\omega|x|)) \tag{2}$$

where $H_0^{(1)}$ and $H_0^{(2)}$ are Hänkel functions of the first and second types.

The MFS uses the fundamental solution to generate particular solutions by shifting the origin—these solutions are called *point-sources*—for instance, the function $\Phi_\omega(\cdot - y)$ is a point-source located at $y \notin \Omega$. The point-sources will be located on some admissible source set (e.g. [5]). For instance, when Ω is bounded and simply connected, we can take the boundary $\hat{\Gamma} = \partial\hat{\Omega}$ of an enclosing open set $\hat{\Omega}$ with $\hat{\Omega} \supset \bar{\Omega}$ (Figure 1). Here $\bar{\Omega}$ stands, as usual, for the closure of the open set Ω in the $\mathbb{R}^2$ topology.

The MFS can be directly related to boundary integral equations of the first kind, through the discretization of boundary layer potentials.

DOI: 10.1002/nme

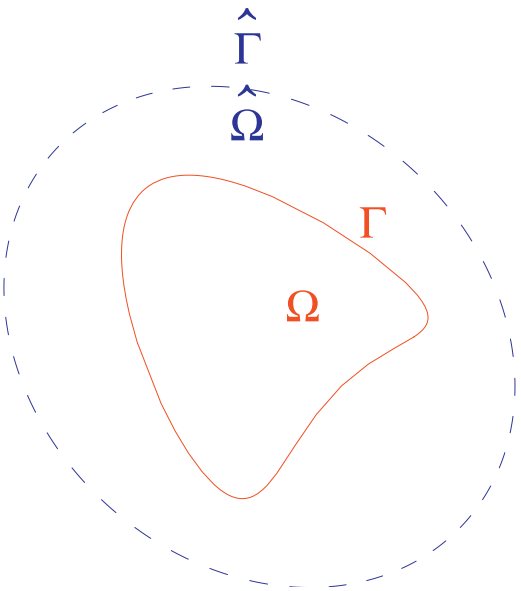

Figure 1. An admissible source set $\hat{\Gamma}$.

Consider the single- and double-layer operators on $\hat{\Gamma}$ (the integrals are defined in the duality sense when the densities are distributions)

$$\mathbf{S}_{\hat{\Gamma}}\phi(x) = \int_{\hat{\Gamma}} \Phi(x-y)\phi(y)\,\mathrm{d}s_y$$

$$\mathbf{D}_{\hat{\Gamma}}\psi(x) = \int_{\hat{\Gamma}} \partial_{n_y}\Phi(x-y)\psi(y)\,\mathrm{d}s_y$$

with $\phi \in H^{-3/2}(\hat{\Gamma})$ and $\psi \in H^{-1/2}(\hat{\Gamma})$. These operators define analytical functions outside $\hat{\Gamma}$, and we will analyse their traces on Γ. We will consider the traces $\gamma^0_\Gamma(u) = u_{|\Gamma}$ and the normal traces $\gamma^n_\Gamma(u) = \partial_n u$ on Γ as $H^{3/2}(\Gamma)$ and $H^{1/2}(\Gamma)$ functions, respectively. This defines a matrix operator $\mathbb{M}_{\hat{\Gamma},\Gamma}: H^{-3/2}(\hat{\Gamma}) \times H^{-1/2}(\hat{\Gamma}) \to H^{3/2}(\Gamma) \times H^{1/2}(\Gamma)$

$$\mathbb{M}_{\hat{\Gamma},\Gamma}(\phi,\psi) = \begin{bmatrix} \gamma^0_\Gamma \mathbf{S}_{\hat{\Gamma}} & \gamma^0_\Gamma \mathbf{D}_{\hat{\Gamma}} \\ \gamma^n_\Gamma \mathbf{S}_{\hat{\Gamma}} & \gamma^n_\Gamma \mathbf{D}_{\hat{\Gamma}} \end{bmatrix} \begin{bmatrix} \phi \\ \psi \end{bmatrix}$$

Theorem 1
If ω is not an eigenfrequency of the interior eigenproblem, then $\mathbb{M}_{\hat{\Gamma},\Gamma}(H^{-3/2}(\hat{\Gamma}) \times H^{-1/2}(\hat{\Gamma}))$ is dense in $H^{3/2}(\Gamma) \times H^{1/2}(\Gamma)$.

Proof
We prove that $\mathrm{Ker}(\mathbb{M}^*_{\hat{\Gamma},\Gamma}) = \{\mathbf{0}\}$ and this implies the density by the Hahn–Banach theorem.

DOI: 10.1002/nme

First, consider the single- and double-layer operators on Γ

$$\mathbf{S}_\Gamma f(y)=\int_\Gamma \Phi(x-y)f(x)\,\mathrm{d}s_x,\quad \mathbf{D}_\Gamma g(y)=\int_\Gamma \partial_{n_y}\Phi(x-y)g(x)\,\mathrm{d}s_x$$

and the adjoints of the trace operators are given by

$$(\gamma_\Gamma^0\mathbf{S}_{\hat\Gamma})^*=\gamma_{\hat\Gamma}^0\mathbf{S}_\Gamma,\quad (\gamma_\Gamma^n\mathbf{S}_{\hat\Gamma})^*=\gamma_{\hat\Gamma}^0\mathbf{D}_\Gamma$$
$$(\gamma_\Gamma^0\mathbf{D}_{\hat\Gamma})^*=\gamma_{\hat\Gamma}^n\mathbf{S}_\Gamma,\quad (\gamma_\Gamma^n\mathbf{D}_{\hat\Gamma})^*=\gamma_{\hat\Gamma}^n\mathbf{D}_\Gamma$$

Thus,

$$\mathbb{M}_{\hat\Gamma,\Gamma}^*=\begin{bmatrix}\gamma_\Gamma^0\mathbf{S}_{\hat\Gamma} & \gamma_\Gamma^0\mathbf{D}_{\hat\Gamma}\\ \gamma_\Gamma^n\mathbf{S}_{\hat\Gamma} & \gamma_\Gamma^n\mathbf{D}_{\hat\Gamma}\end{bmatrix}^*=\begin{bmatrix}\gamma_{\hat\Gamma}^0\mathbf{S}_\Gamma & \gamma_{\hat\Gamma}^0\mathbf{D}_\Gamma\\ \gamma_{\hat\Gamma}^n\mathbf{S}_\Gamma & \gamma_{\hat\Gamma}^n\mathbf{D}_\Gamma\end{bmatrix}=\mathbb{M}_{\Gamma,\hat\Gamma}$$

Take $u=\mathbf{S}_\Gamma f+\mathbf{D}_\Gamma g$, an analytic function defined outside Γ; then $\mathbb{M}_{\hat\Gamma,\Gamma}^*(f,g)=(\gamma_{\hat\Gamma}^0u,\gamma_{\hat\Gamma}^nu)=(u,\partial_nu)_{|\hat\Gamma}$. Thus, to prove that $\mathrm{Ker}(\mathbb{M}_{\hat\Gamma,\Gamma}^*)=\{\mathbf{0}\}$ it is sufficient to prove that $u=\partial_nu=0$ on $\hat\Gamma$ implies $f=g=0$.

It is clear that if $u=\partial_nu=0$ on $\hat\Gamma$ we have an exterior eigenvalue problem in $\mathbb{R}^2\backslash\bar{\hat\Omega}$ and by the well posedness of the exterior problem, adding the radiation condition

$$\lim_{|x|\to\infty}\left(\frac{\partial u(x)}{\partial|x|}-\mathrm{i}\lambda u(x)\right)=o(|x|^{-1/2})$$

which is satisfied (cf. [18]) by these operators, we have $u=0$ in $\mathbb{R}^2\backslash\bar{\hat\Omega}$. Since u is analytic outside Γ, by analytic extension, $u\equiv0$ in $\mathbb{R}^2\backslash\bar\Omega$.

Now, using the continuity of the first traces of $\mathbf{S}_\Gamma$ and $\mathbf{D}_\Gamma$ on Γ (cf. [18]), we have (superscript $+$ denotes exterior and $-$ denotes interior)

$$u^-=u^+=0,\quad \partial_nu^-=\partial_nu^+=0$$

Therefore, u verifies the eigenvalue bilaplacian equation in the interior Ω with null boundary Dirichlet conditions $u^-=\partial_nu^-=0$. If ω^4 is not an eigenvalue then the solution is unique and this implies $u\equiv0$ in Ω. We conclude that $u\equiv0$ in $\mathbb{R}^2\backslash\Gamma$ and moreover, using the jump relations for the other traces (cf. [18]), $f=(\partial_n\Delta u)^--(\partial_n\Delta u)^+=0$ and $g=(\Delta u)^+-(\Delta u)^-=0$. □

Matrix $\mathbb{M}_{\hat\Gamma,\Gamma}$ depends on the fundamental solutions and in particular on ω; therefore, we will express $\mathbb{M}_{\hat\Gamma,\Gamma}(\omega)$ to enhance this dependence. Using the previous result, we will search for the frequencies ω such that $\dim(\mathrm{Ker}(\mathbb{M}_{\hat\Gamma,\Gamma}(\omega)))\neq0$. These frequencies will give the eigenvalues ω^4 of the bilaplacian–Dirichlet operator and a function $\psi\in\mathrm{Ker}(\mathbb{M}_{\hat\Gamma,\Gamma}(\omega))\backslash\{\mathbf{0}\}$ will be an eigenfunction associated with ω^4.

DOI: 10.1002/nme

3. NUMERICAL METHOD USING THE MFS

3.1. Determination of the eigenfrequencies

From the previous considerations we consider particular solutions of the eigenvalue biharmonic equation, $\Delta^2 u - \omega^4 u = 0$, expressed with boundary integral operators ($x \in \Omega$)

$$u(x) = \int_{\hat{\Gamma}} \Phi_\omega(x-y)\varphi(y)\,\mathrm{d}s_y + \int_{\hat{\Gamma}} \partial_{n_y}\Phi_\omega(x-y)\psi(y)\,\mathrm{d}s_y$$

with unknown densities φ and ψ. A discretization of these integrals (that are regular, since $x \in \Omega$ and $\hat{\Gamma} \cap \Omega = \emptyset$) is not required, and we just take the linear combinations

$$u_m(x) = \sum_{j=1}^{m} \alpha_{m,j}\Phi_\omega(x-y_{m,j}) + \sum_{j=1}^{m} \beta_{m,j}\partial_{n_{y_{m,j}}}\Phi_\omega(x-y_{m,j}) \tag{3}$$

where the coefficients $\alpha_{m,j}$ and $\beta_{m,j}$ can be seen to include the integration weights ($y_{m,j} \in \hat{\Gamma}$ being the integration points). These functions u_m are still particular solutions, and instead of retrieving the continuous densities, it is sufficient to fit the boundary conditions by changing the unknown coefficients. In addition, ∂_{n_y} the normal derivative at a point $y \in \hat{\Gamma}$, does not need to be precisely calculated, since the curve $\hat{\Gamma}$ is artificial.

By choosing collocation points $x_1, \ldots, x_m \in \Gamma$, the null Dirichlet boundary conditions lead to the $(2m) \times (2m)$ system

$$\begin{aligned} 0 = u_m(x_i) &= \sum_{j=1}^{m} \alpha_{m,j}\Phi_\omega(x_i - y_{m,j}) + \sum_{j=1}^{m} \beta_{m,j}\partial_{n_{y_{m,j}}}\Phi_\omega(x_i - y_{m,j}) \\ 0 = \partial_{n_{x_i}} u_m(x_i) &= \sum_{j=1}^{m} \alpha_{m,j}\partial_{n_{x_i}}\Phi_\omega(x_i - y_{m,j}) + \sum_{j=1}^{m} \beta_{m,j}\partial_{n_{x_i}}\partial_{n_{y_{m,j}}}\Phi_\omega(x_i - y_{m,j}) \end{aligned} \tag{4}$$

We then search for the frequencies ω for which the system is not invertible (discretized version of $\dim(\mathrm{Ker}(\mathbb{M}_{\hat{\Gamma},\Gamma}(\omega))) \neq 0$).

Algorithm to choose the point-sources. As described in [7], an arbitrary choice of source-points may lead to worst results than the expected with the MFS applied to simple shapes.

We will proceed with the following algorithm:

(i) Uniform distribution of the collocation points $x_1, \ldots, x_m \in \Gamma$ such that $|x_k - x_{k+1}| \approx |x_k - x_{k-1}| = \varepsilon$.

(ii) For each x_k calculate an approximation for the unitary vector n_{x_k} (for small $\varepsilon \approx 0$, $n_{x_k} \times (x_{k+1} - x_{k-1}) \approx 0$).

(iii) Define as point-sources

$$y_k = x_k + \beta n_{x_k}$$

where β is an experimental value. A small β gives better conditioning but worst approximations. Higher values of β can be used when the boundary Γ is more or less trivial. The parameter β must be such that $y_j \notin \Omega$, $j = 1, \ldots, m$ (check [7] for details), and with this restriction, this choice could also be applied for multiply connected shapes.

(iv) Assume that $n_{y_{m,j}} = n_{x_j}$ and denote this vector simply by n_j.

DOI: 10.1002/nme

With these choices the point-sources may define an artificial $\hat{\Gamma}$ curve that follows the original shape of the boundary Γ. Thus, this algorithm does not follow exactly the theoretical argument, where the $\hat{\Gamma}$ curve was fixed. Since the number of point-sources is finite, it would be possible to consider an artificial continuous $\hat{\Gamma}$ that would include all the points in this construction; however, it is not in our numerical purpose to follow exactly the theoretical argument. On the other hand, since this distribution of point-sources follows the positioning of the collocation points, the diagonal of the system matrix becomes more dominant (for sufficiently small β it would be dominant) and this may explain the better conditioning (results with different choices of source-points are plotted in Figure 5; the proposed choice leads to the regular curve on the right).

Using the notation $d_{i,j} = x_i - y_{m,j}$ system (9) becomes

$$\begin{aligned} 0 &= \sum_{j=1}^{m} \alpha_{m,j} \Phi_\omega(d_{i,j}) + \sum_{j=1}^{m} \beta_{m,j} (n_j \cdot \nabla \Phi_\omega(d_{i,j})) \\ 0 &= \sum_{j=1}^{m} \alpha_{m,j} (n_i \cdot \nabla \Phi_\omega(d_{i,j})) + \sum_{j=1}^{m} \beta_{m,j} (n_i \cdot \nabla (n_j \cdot \nabla \Phi_\omega(d_{i,j}))) \end{aligned} \tag{5}$$

Therefore, a straightforward procedure is to find the values ω for which the $(2m) \times (2m)$ matrix $\mathbf{M}_m(\omega)$ has a null determinant:

$$\mathbf{M}_m(\omega) = \begin{bmatrix} [A(\omega)]_{m\times m} & [B(\omega)]_{m\times m} \\ [C(\omega)]_{m\times m} & [D(\omega)]_{m\times m} \end{bmatrix}_{2m\times 2m} \tag{6}$$

This matrix is composed of the following four $m \times m$ blocks:

$$\begin{aligned} A(\omega) &= [\Phi_\omega(d_{i,j})]_{m\times m}, \quad B(\omega) = [n_j \cdot \nabla \Phi_\omega(d_{i,j})]_{m\times m} \\ C(\omega) &= [n_i \cdot \nabla \Phi_\omega(d_{i,j})]_{m\times m}, \quad D(\omega) = [n_i \cdot \nabla (n_j \cdot \nabla \Phi_\omega(d_{i,j}))]_{m\times m} \end{aligned}$$

Remark 1

As described in [12], one possibility of reducing the dimension of the system matrix is to calculate the matrix $\mathbf{N}(\omega) = C - D.B^{-1}.A$. This reduces the dimension of the system matrix from $(2m) \times (2m)$ to $m \times m$; however, we preferred to avoid the calculation of the inverse matrix B^{-1}.

The components of the matrix $\mathbf{M}_m(\omega)$ are complex numbers; hence, the determinant is also a complex number.

We consider the real function

$$g(\omega) = |\det[\mathbf{M}_m(\omega)]|$$

and search for the local minima of this function. It is clear that the function g will be very small in any case, since the MFS is highly ill-conditioned and the determinants are always very small. Using $\log(g(\omega))$ the null determinant would lead to a singularity—see the graph plot in Figure 2.

Finally, to search the point where a local minimum is attained we used an algorithm based on the *golden ratio search method* (see [7] for details).

DOI: 10.1002/nme

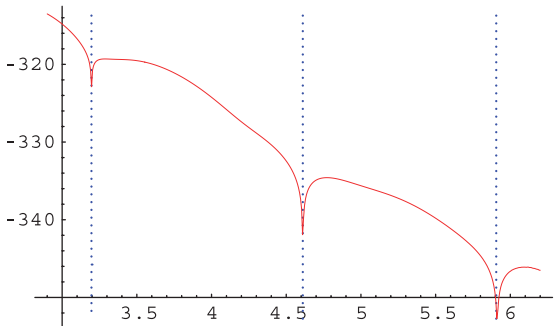

Figure 2. Plot of the graph of $\log(g(\omega))$ for the circle.

3.2. *Determination of the eigenmodes*

To obtain an eigenmode associated with a certain approximation for an eigenfrequency $\tilde{\lambda}$, we use a collocation method on $m+1$ points, with $x_1, \ldots, x_m$ on Γ, a point $x_{m+1} \in \Omega$ and an extra point-source $y_{m+1} \in \bar{\Omega}^C$. The approximation of the eigenmode is given by

$$\tilde{u}(x) = \sum_{j=1}^{m+1} \alpha_{m+1,j} \Phi_{\tilde{\lambda}}(x - y_{m+1,j}) + \sum_{j=1}^{m} \beta_{m,j} \partial_{n_{y_{m,j}}} \Phi_{\tilde{\lambda}}(x - y_{m,j}) \tag{7}$$

To exclude the solution $\tilde{u}(x) \equiv 0$, the coefficients $\alpha_{m+1,j}$ and $\beta_{m,j}$ are obtained by solving the system

$$\begin{cases} \tilde{u}(x_i) = 0, & i = 1, \ldots, m \\ \tilde{u}(x_{m+1}) = 1 \\ \partial_n \tilde{u}(x_i) = 0, & i = 1, \ldots, m \end{cases} \tag{8}$$

This is equivalent to solving the $(2m+1) \times (2m+1)$ system

$$\begin{bmatrix} [A(\omega)]_{m \times (m+1)} & [B(\omega)]_{m \times m} \\ [\Phi_{\tilde{\lambda}}(d_{m+1,j})]_{1 \times (m+1)} & [0]_{1 \times m} \\ [C(\omega)]_{m \times (m+1)} & [D(\omega)]_{m \times m} \end{bmatrix} \begin{bmatrix} [\alpha_{m+1,j}]_{(m+1) \times 1} \\ [\beta_{m,j}]_{m \times 1} \end{bmatrix} = \begin{bmatrix} [0]_{m \times 1} \\ 1 \\ [0]_{m \times 1} \end{bmatrix} \tag{9}$$

Remark 2

Depending on the multiplicity of the eigenvalue, we can add one or more collocation points to make the linear system well determined. This procedure allows us to determine the eigenspace, with an appropriate iterative choice of values. A similar procedure was considered in [19]. The procedure may fail if the selected point x_{m+1} is on a nodal line (cf. [20]), but this can be easily circumvented with a random choice, since the nodal lines have null Lebesgue measure in $\mathbb{R}^2$.

DOI: 10.1002/nme

3.3. Numerical algorithms

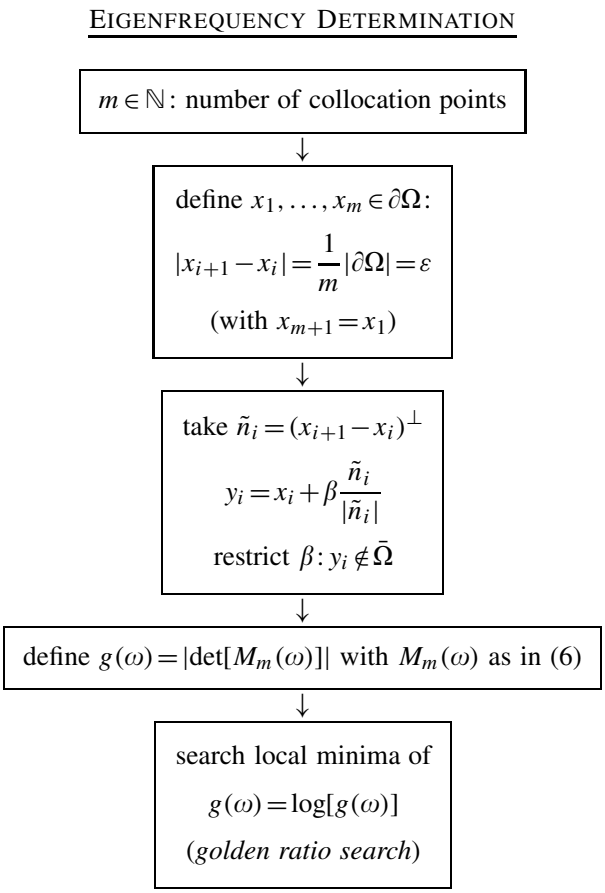

Algorithm 1: *Flow chart for the eigenfrequency determination algorithm.*

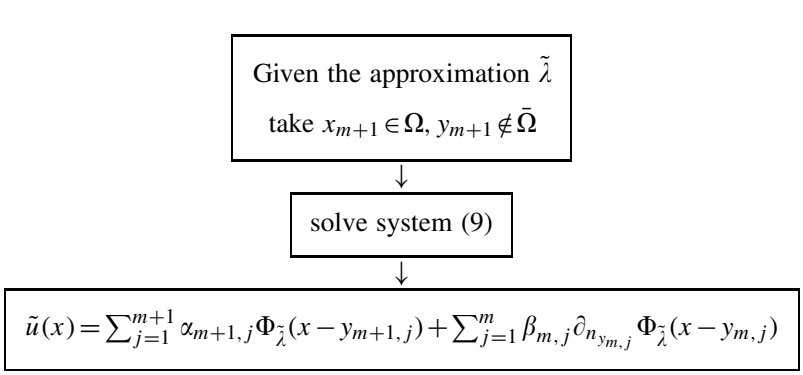

Algorithm 2: *Flow chart for the eigenmode calculation algorithm.*

DOI: 10.1002/nme

3.4. Error bounds

We recall a result that was attributed by Collatz (cf. [21]) to Kryloff and Bogoliubov and to D. H. Weinstein.

Theorem 2
Let A be a self-adjoint operator on a Hilbert space with inner product $\langle \cdot, \cdot \rangle$. Let λ_n and u_n be the eigenvalues and orthonormal eigenfunctions of A and assume that the sequence $\{\lambda_n\}$ has no finite accumulation point. Let v be any element in the space spanned by $\{u_n\}$ and let

$$\rho = \frac{\langle v, Av \rangle}{\|v\|^2} \quad \text{(the Rayleigh quotient)}$$

and

$$\sigma = \frac{\|Av\|}{\|v\|}$$

Then $\sigma \geqslant \rho$ and there exists at least one eigenvalue λ satisfying

$$\rho - \sqrt{\sigma^2 - \rho^2} \leqslant \lambda \leqslant \rho + \sqrt{\sigma^2 - \rho^2}$$

Proof
See [11]. □

Applying the previous result to the biharmonic operator, we can present an error estimate for the results obtained with the MFS (or other methods based on particular solutions).

Theorem 3
Consider Ω a bounded domain with a regular boundary (piecewise C^1). Let $\tilde{\lambda}$ and $\tilde{u} \in C^4(\Omega) \cap C^1(\bar{\Omega})$ be approximate values for an eigenfrequency λ and an eigenfunction u (respectively) such that

$$\begin{cases} \Delta^2 \tilde{u} - \tilde{\lambda}^4 \tilde{u} = 0 & \text{in } \Omega \\ \tilde{u} = e_0 & \text{on } \partial\Omega \\ \partial_n \tilde{u} = e_1 & \text{on } \partial\Omega \end{cases} \tag{10}$$

with $\|\tilde{u}\|_{L^2(\Omega)} = 1$. Consider e to be the solution of the homogeneous problem $\Delta^2 e = 0$, in Ω, with boundary conditions $e = e_0, \partial_n e = e_1$, on $\partial\Omega$. The boundary functions e_0 and e_1 are assumed to be sufficiently small such that $\varepsilon = \|e\|_{L^2(\Omega)} < 1$. Then there exists an eigenfrequency λ such that

$$\left| \frac{\lambda^4 - \tilde{\lambda}^4}{\tilde{\lambda}^4} \right| \leqslant \frac{\sqrt{2}\varepsilon + \varepsilon^2}{(1-\varepsilon)^2}$$

Proof
Let $v = \tilde{u} - e$, with

$$\begin{cases} \Delta^2 e = 0 & \text{in } \Omega \\ e = e_0 & \text{on } \partial\Omega \\ \partial_n e = e_1 & \text{on } \partial\Omega \end{cases} \quad \text{then} \quad \begin{cases} \Delta^2 v = \tilde{\lambda}^4 \tilde{u} & \text{in } \Omega \\ v = 0 & \text{on } \partial\Omega \\ \partial_n v = 0 & \text{on } \partial\Omega \end{cases} \tag{11}$$

DOI: 10.1002/nme

For the regular bounded shapes Ω, the bilaplacian eigenvalue problem is well posed except for a discrete sequence of positive eigenvalues, which accumulates at infinity. Since v verifies the boundary conditions, we can write it in the span$\{u_n\}$, in the conditions of Theorem 2 with $A=\Delta^2$.

Table I. Absolute errors for the circle.

m	Absolute error (λ_1)	m	Absolute error (λ_2)	m	Absolute error (λ_3)
20	4.23176×10^{-6}	20	7.88573×10^{-5}	20	5.54069×10^{-3}
25	4.17119×10^{-8}	25	8.80722×10^{-7}	25	7.58151×10^{-5}
30	3.66573×10^{-10}	30	3.85887×10^{-8}	30	3.57842×10^{-6}

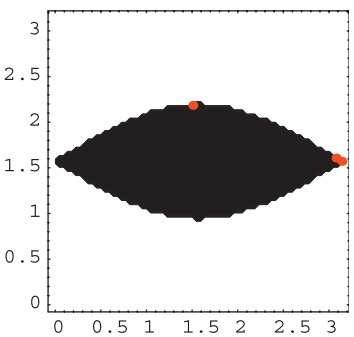

Figure 3. Domain 2.

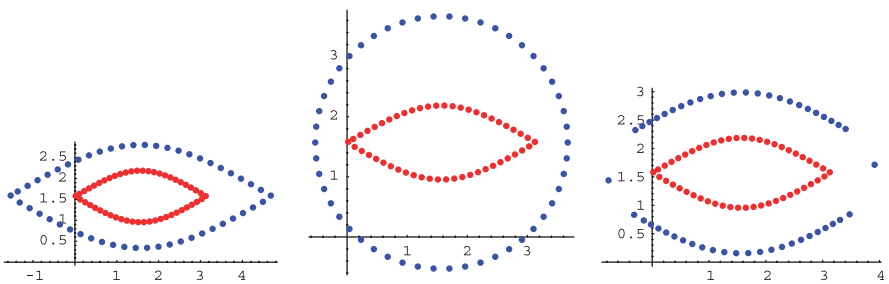

Figure 4. Collocation points and three different choices for the point-sources with $m=70$.

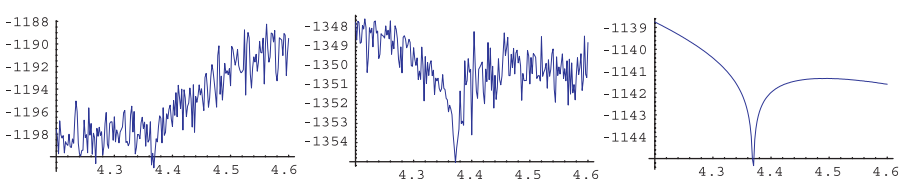

Figure 5. Plot of the function $\log(g(\omega))$ with $m=70$ for three choices of points.

DOI: 10.1002/nme

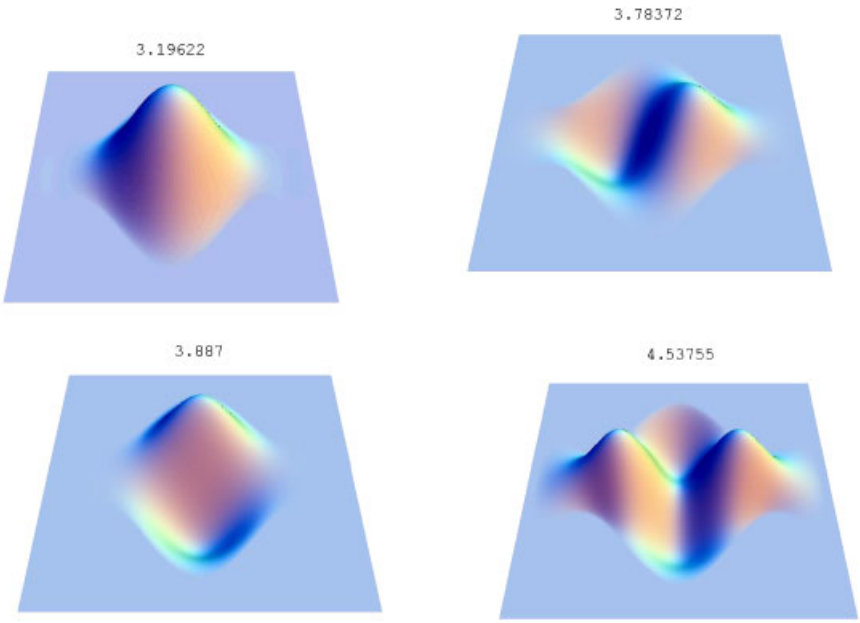

Figure 6. Plots of eigenmodes associated with the first four eigenfrequencies of the domain Ω_2.

Thus, there exists an eigenvalue λ^4 such that

$$|\lambda^4-\rho_A(v)|\leqslant\sqrt{\rho_{A^2}(v)-\rho_A(v)^2}$$

The Rayleigh quotient for v is now given by

$$\rho_A(v)=\frac{\langle v,\Delta^2 v\rangle}{\|v\|^2}=\tilde{\lambda}^4\frac{\langle v,\tilde{u}\rangle}{\|v\|^2}$$

and assuming $\varepsilon<1$ we see that $\rho_A(v)$ is relatively close to $\tilde{\lambda}^4$,

$$\frac{\rho_A(v)-\tilde{\lambda}^4}{\tilde{\lambda}^4}=\frac{\langle v,e\rangle}{\|v\|^2}=\frac{\langle e,\tilde{u}\rangle-\|e\|^2}{\|v\|^2}$$

On the other hand, we have

$$\rho_{A^2}(v)=\frac{\langle\Delta^2 v,\Delta^2 v\rangle}{\|v\|^2}=\frac{\tilde{\lambda}^8}{\|v\|^2}$$

Since $\langle v,v\rangle-\langle v,\tilde{u}\rangle^2=(1-2\langle e,\tilde{u}\rangle+\|e\|^2)-(1-2\langle e,\tilde{u}\rangle+\langle e,\tilde{u}\rangle^2)=\|e\|^2-\langle e,\tilde{u}\rangle^2$, we have

$$\left|\frac{\lambda^4-\rho_A(v)}{\tilde{\lambda}^4}\right|\leqslant\frac{1}{\tilde{\lambda}^4}\sqrt{\rho_{A^2}(v)-\rho_A(v)^2}=\frac{1}{\|v\|^2}\sqrt{\|v\|^2-\langle v,\tilde{u}\rangle^2}\leqslant\frac{1}{\|v\|^2}\sqrt{\|e\|^2-\langle e,\tilde{u}\rangle^2}$$

DOI: 10.1002/nme

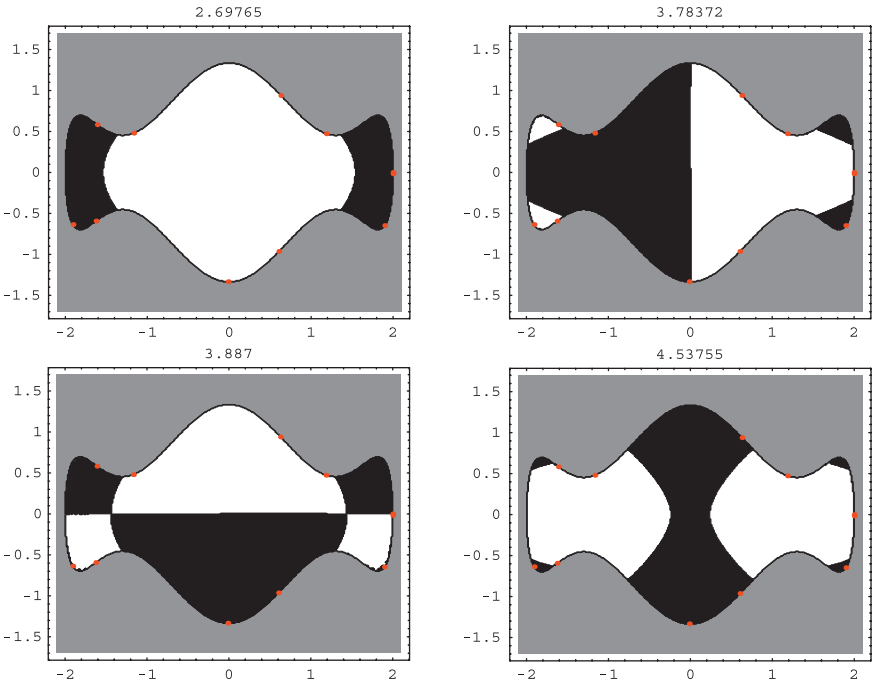

Figure 7. Nodal domains of the eigenmodes associated with the first four eigenfrequencies of the domain Ω_2.

Thus

$$\left|\frac{\lambda^4-\tilde{\lambda}^4}{\tilde{\lambda}^4}\right| \leqslant \left|\frac{\lambda^4-\rho_A(v)}{\tilde{\lambda}^4}\right| + \left|\frac{\rho_A(v)-\tilde{\lambda}^4}{\tilde{\lambda}^4}\right| \leqslant \frac{|\|e\|^2-\langle e,\tilde{u}\rangle| + \sqrt{\|e\|^2-\langle e,\tilde{u}\rangle^2}}{\|v\|^2}$$

Using the trivial bounds $|\|e\|^2-\langle e,\tilde{u}\rangle| \leqslant \|e\|^2+\|e\|$, $\|e\|^2-\langle e,\tilde{u}\rangle^2 \leqslant \|e\|^2$ and $(1-\|e\|)^2 \leqslant \|v\|^2$, we get

$$\left|\frac{\lambda^4-\tilde{\lambda}^4}{\tilde{\lambda}^4}\right| \leqslant \|e\|\frac{2+\|e\|}{(1-\|e\|)^2}$$

It is also possible to sharpen the previous estimate by noticing that $\pm\alpha+\sqrt{1-\alpha^2} \leqslant \sqrt{2}$ with $|\alpha| = |\langle \tilde{e},\tilde{u}\rangle| \leqslant 1$ and $\tilde{e} = e/\|e\|$. □

Remark 3

The previous estimate depends on the domain norm $\varepsilon = \|e\|_{L^2(\Omega)}$ as an $O(\varepsilon)$. It is also clear that we can relate it directly to the boundary values by the well posedness of the bilaplacian problem. For instance, using Theorem 3.2 of [22] we obtain

$$\|e\|_{L^2(\Omega)} \leqslant (\|\varepsilon_0\|_{L^2(\partial\Omega)} + \|\partial_\tau \varepsilon_0\|_{L^2(\partial\Omega)} + \|\varepsilon_1\|_{L^2(\partial\Omega)}) c_\Omega$$

where c_Ω depends only on the domain.

DOI: 10.1002/nme

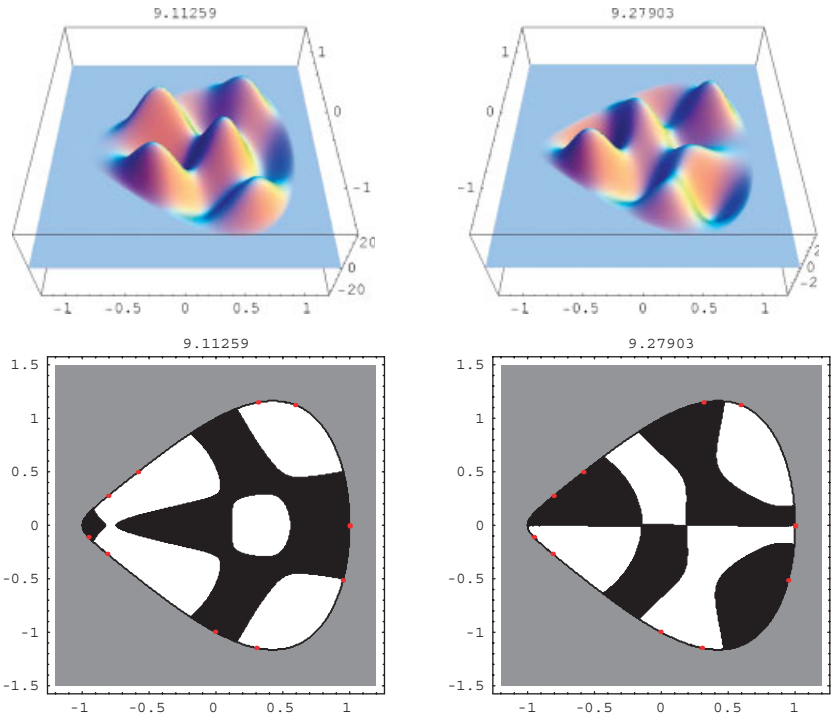

Figure 8. Plots of eigenmodes and the respective nodal domains associated with the 14th and 16th eigenfrequencies of the domain Ω_3.

4. NUMERICAL RESULTS

In Figure 2 we plot the graph of $\log(g(\omega))$, $\omega \in [2.9, 6.2]$ for the circle obtained with $m = 15$ and $\beta = 1.5$.

In Table I we present the results of the absolute errors for the circle (with $\beta = 1.5$). Now we test the method for the domain with boundary given implicitly by

$$\sin^2(y) + \tfrac{1}{3}\sin^2(x) = 1$$

We obtain the domain plotted in Figure 3. We will now consider three cases of different choices for the point-sources. In the first case, we consider as artificial boundary the 'expansion' of the boundary of the domain; in the second case, we consider the boundary of a circular domain and in the last case we consider the choice proposed with $\beta = 0.8$ (Figure 4).

In Figure 5 we present the plot of $\log(g(\omega))$ with the points plotted in Figure 4. We note that in Figure 5 the first two plots present rounding errors generated by the ill-conditioned matrix. With the proposed choice of points, the ill-conditioning decreases and the rounding errors are much smaller (third plot). This phenomenon also occurs in the membrane problem (cf. [7]).

DOI: 10.1002/nme

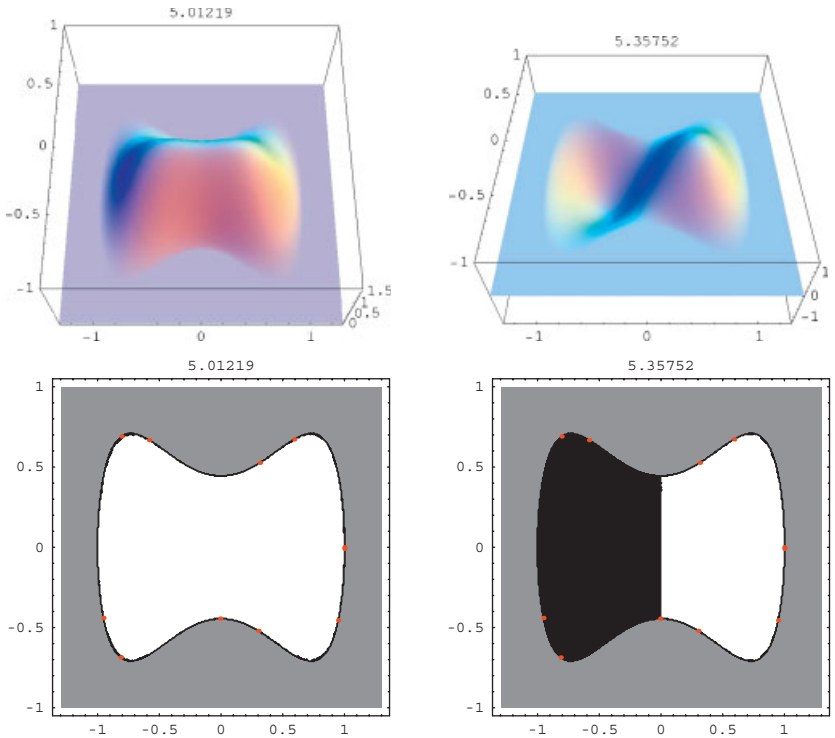

Figure 9. Plots of eigenmodes and the respective nodal domains associated with the first and second eigenfrequencies of the domain Ω_4.

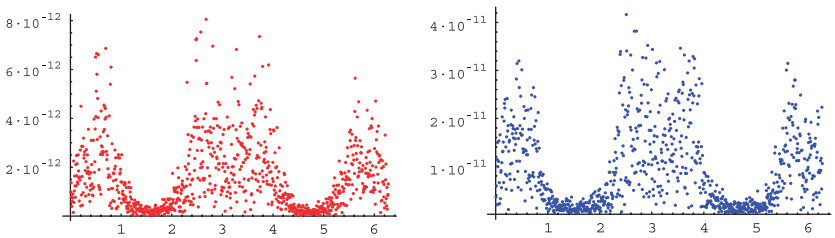

Figure 10. Plot of $\tilde{u}|_{\partial\Omega}$ and $\partial_n \tilde{u}|_{\partial\Omega}$ for the eigenmode associated with the first eigenfrequency of the domain Ω_4.

We will denote by the domains Ω_2, Ω_3 and Ω_4, which can be parametrized (respectively) by

$$t \mapsto \left(2\cos(t), \sin(t) + \frac{\sin(5t)}{3}\right)$$

DOI: 10.1002/nme

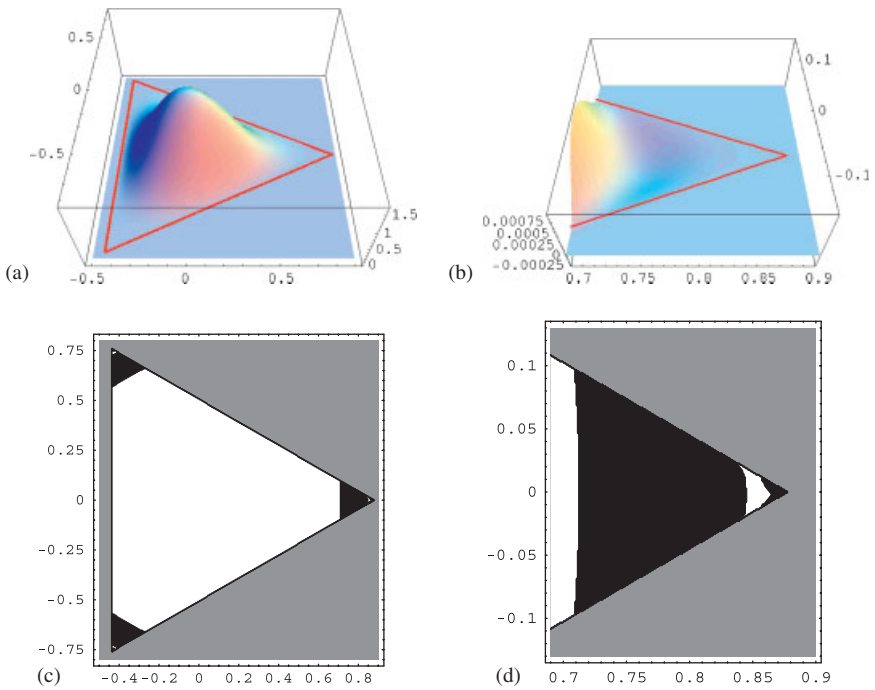

Figure 11. (a) Plot of the eigenmode associated with the first eigenfrequency; (b) zoom of the behaviour of the eigenmode near the right corner; (c) the nodal domains; and (d) the nodal domain near the right corner.

and

$$t \mapsto \left(\cos(t), \sin(t) + \frac{\sin(2t)}{3}\right)$$

$$t \mapsto \left(\cos(t), \sin(t) + \frac{5\sin(t)\cos(2t)}{9}\right)$$

In Figure 6 we plot the eigenmodes associated with the first four eigenfrequencies of the domain Ω_2. In Figure 7 we plot the respective nodal domains. In Figure 8 we plot the eigenmodes and the respective nodal domains associated with the 14th and 16th eigenfrequencies of the domain Ω_3.

In Figure 9 we plot the eigenmodes and the respective nodal domains associated with the first and second eigenfrequencies of the domain Ω_4.

Using Theorem 3 we can obtain bounds for the errors of the approximation of the eigenfrequency, which are very good if the functions $\varepsilon(x)$ and $\delta(x)$ are sufficiently small on the boundary. In Figure 10 we plot $\tilde{u}|_{\partial\Omega}$ and $\partial_n\tilde{u}|_{\partial\Omega}$ for the eigenmode associated with the first eigenfrequency of the domain Ω_4.

It is well known that the eigenmode associated with the first eigenfrequency of the laplacian in a domain Ω does not change the sign in Ω. For the bilaplacian it was proven that this is not true (cf. [23, 24]). For some polygonal domains with a corner with sufficiently small internal angle θ, any eigenmode changes the sign an infinite number of times in the neighbourhood of this corner.

DOI: 10.1002/nme

One of these domains is the equilateral triangle. We will consider the equilateral triangle with vertices $\{(-\frac{1}{2}, \sqrt{3}/2), (-\frac{1}{2}, -\sqrt{3}/2), \ (1,0)\}/(3^{3/4}/2)$ which has unit area. In Figure 11 we plot the eigenmode associated with the first eigenfrequency of the equilateral triangle, the respective nodal domains and the behaviour (and nodal domains) of the eigenmode near one of the corners.

5. CONCLUSIONS

In this paper we justified the application of the method of fundamental solutions (MFS) as a solver for the clamped plate eigenvalue problem, by proving density results and presenting error estimates that allow one to control the approximation of the eigenvalue from the boundary approximation given by the MFS. To circumvent the problem of ill-conditioning, we propose a particular choice for the collocation points and point-sources as in [7] that revealed to be important to solve accurately these eigenproblems for non-trivial domains. We addressed the simply connected clamped plate, but under appropriate modifications the method can be extended for the multiply connected case (cf. [17]) and to other boundary conditions (cf. [15] for the unit circle).

ACKNOWLEDGEMENTS

This study was partially supported by FCT-POCTI/FEDER, project POCTI-MAT/34735/00, POCTI-MAT/60863/2004, POCTI-ECM/58940/2004 and NATO-PST.CLG.980398. Pedro Antunes is also partially supported by Fundação para a Ciência e Tecnologia through the scholarship SFRH/BD/19879/2004.

REFERENCES

1. Mey GDe. Calculation of the eigenvalues of the Helmholtz equation by an integral equation. *International Journal for Numerical Methods in Engineering* 1976; **10**:59–66.
2. Betcke T, Trefethen LN. Reviving the method of particular solutions. *SIAM Review* 2005; **47**:469–491.
3. Kupradze VD, Aleksidze MA. The method of functional equations for the approximate solution of certain boundary value problems. *U.S.S.R. Computational Mathematics and Mathematical Physics* 1964; **4**:82–126.
4. Karageorghis A. The method of fundamental solutions for the calculation of the eigenvalues of the Helmholtz equation. *Applied Mathematics Letters* 2001; **14**(7):837–842.
5. Alves CJS, Chen CS. A new method of fundamental solutions applied to nonhomogeneous elliptic problems. *Advances in Computational Mathematics* 2005; **23**:125–142.
6. Alves CJS, Silvestre AL. Density results using Stokeslets and a method of fundamental solutions for the Stokes equations. *Engineering Analysis with Boundary Elements* 2004; **28**:1245–1252.
7. Alves CJS, Antunes PRS. The method of fundamental solutions applied to the calculation of eigenfrequencies and eigenmodes of 2D simply connected shapes. *Computers*, *Materials and Continua* 2005; **2**(4):251–266.
8. Chen JT, Chen IL, Lee YT. Eigensolutions of multiply connected membranes using the method of fundamental solutions. *Engineering Analysis with Boundary Elements* 2005; **29**(2):166–174.
9. Tsai CC, Young DL, Chen CW, Fan CM. The method of fundamental solutions for eigenproblems in domains with and without interior holes. *Proceedings of the Royal Society of London*, *Series A* 2006; **462**:1443–1466.
10. Chen JT, Chang MH, Chen KH, Lin SR. Boundary collocation method with meshless concept for acoustic eigenanalysis of two-dimensional cavities using radial basis function. *Journal of Sound and Vibration* 2002; **257**(4):667–711.
11. Fox L, Henrici P, Moler CB. Approximations and bounds for eigenvalues of elliptic operators. *SIAM Journal on Numerical Analysis* 1967; **4**:89–102.
12. Kang SW, Lee JM. Free vibration analysis of arbitrary shaped plates with clamped edges using wave-type functions. *Journal of Sound and Vibration* 2001; **242**(1):9–16.

DOI: 10.1002/nme

13. Chen JT, Chen IL, Chen KH, Lee YT, Yeh YT. A meshless method for free vibration analysis of circular and rectangular clamped plates using radial basis function. *Engineering Analysis with Boundary Elements* 2004; **28**:535–545.
14. Chen KH, Chen JT, Kao JH. Regularized meshless method for solving acoustic eigenproblem with multiply-connected domain. *Computer Modeling in Engineering and Sciences* 2006; **16**(1):27–39.
15. Young DL, Tsai CC, Lin YC, Chen CS. The method of fundamental solutions for eigenfrequencies of plate vibrations. *Computers*, *Materials and Continua* 2006; **4**(1):1–10.
16. Lee WM, Chen JT, Lee YT. Free vibration analysis of circular plates with multiple circular holes using indirect BIEMs. *Journal of Sound and Vibration* 2007; **304**:811–830.
17. Chen JT, Lee YT. True and spurious eigensolutions for membrane and plate problems by using the method of fundamental solutions. *ECCOMAS Thematic Conference on Meshless Methods*, Lisbon, 2005.
18. Kitahara M. *Boundary Integral Equation Methods in Eigenvalue Problems of Elastodynamics and Thin Plates*. Elsevier: Amsterdam, 1985.
19. Chen JT, Chen KH, Chyuan SW. Numerical experiments for acoustic modes of a square cavity using the dual BEM. *Applied Acoustics* 1999; **57**(4):293–325.
20. Chen JT, Huang CX, Chen KH. Determination of spurious eigenvalues and multiplicities of the true eigenvalues using the real-part BEM. *Computational Mechanics* 1999; **24**(1):41–51.
21. Collatz L. *Eigenwertprobleme und ihre Numerische Behandlung*. Akademische Verlagsgesellschaft: Leipzig, 1945; 208.
22. Dahlberg BEJ, Kenig CE, Verchota GC. The Dirichlet problem for the biharmonic equation in a Lipschitz domain. *Annales de l'Institut Fourier*, *Grenoble* 1986; **36**:109–135.
23. Blum H, Rannacher R. On the boundary value problem of the biharmonic operator on domains with angular corners. *Mathematical Methods in the Applied Sciences* 1980; **2**:556–581.
24. Coffman CV. On the structure of solutions $\Delta^2 u = \lambda u$ which satisfy the clamped plate conditions on a right angle. *SIAM Journal on Mathematical Analysis* 1982; **13**:746–757.

DOI: 10.1002/nme